ISSN 1070-4272, Russian Journal of Applied Chemistry, 2015, Vol. 88, No. 9, pp. 1417−1427. © Pleiades Publishing, Ltd., 2015.
Original Russian Text © L.N. Maskaeva, A.I. Shemyakinaa, V.F. Markov, R.Kh. Saryeva, 2015, published in Zhurnal Prikladnoi Khimii, 2015, Vol. 88, No. 9, pp. 1271−1281.

INORGANIC SYNTHESIS AND INDUSTRIAL INORGANIC CHEMISTRY

Prognostication of Chemical Deposition Conditions and Morphology of Nanostructured Zinc Sulfide Films

L. N. Maskaeva[a,b], A. I. Shemyakina[a], V. F. Markov[a,b], and R. Kh. Saryeva[a]

[a] *Ural Federal University named after B.N. Yeltsin, ul. Mira 19, Yekaterinburg, 620002 Russia*
[b] *Ural Institute of the State Fire Service of the Ministry of Emergency Situation of Russia, ul. Mira 22, Yekaterinburg, 620062 Russia*
e-mail: mln@ural.ru

Received May 21, 2015

Abstract—Ionic equilibria in the systems Zn^{2+}–$C_6H_5O_7^{3-}$ and Zn^{2+}–NH_3–OH^- were analyzed and boundary conditions and formation regions of ZnS and accompanying impurity phases $Zn(OH)_2$ and $ZnCN_2$ were determined. The hydrochemical method was used to synthesize nanocrystalline zinc sulfide films with thicknesses of 200–240 nm. The scanning electron microscopy demonstrated the influence exerted by complexing agents, nature of a zinc salt, substrate material, and process temperature on the microstructure and morphology of the ZnS layers synthesized. The nanostructured ZnS films have a B3 cubic structure (sphalerite type, space group $F\bar{4}3m$).

DOI: 10.1134/S1070427215090062

Zinc sulfide ZnS a III–VI binary semiconductor with good transparency in a wide wavelength range, low reflectance, and high chemical resistance and thermal stability, attracts increased researchers' attention. Owing to the combination of these properties, ZnS is widely used in laser technology as an active and passive element and is promising for use in nanoelectronics and nanophotonics [1, 2].

Being advantageous over CdS in delivery of high-energy photons to the absorbing material, ZnS makes higher the short-circuit current in solar cells and can replace cadmium sulfide in CdTe/CdS and CdS/CIGS (CIGS is copper indium gallium selenide) heterostructures and serve as a component of cascaded photovoltaic cells [3–5]. For example, replacement of the conventional CdS window layer in *n*-CdS/*p*-CdTe heterostructures with a wider bandgap ZnS results in that the efficiency of photovoltaic converters increases by nearly 1.5% [6].

At present, the compound Cu_2ZnSnS_4 (CZTS) with a kesterite structure is regarded as one of the most promising, in a number of parameters, materials for solar photovoltaic converters [7]. Zinc sulfide is one of the basic semiconductor compounds in this material. It is noteworthy that, owing to the application of the kinetic-thermodynamic approach, both powders and films of another basic sulfide in the CZTS composition, tin sulfide SnS, have been deposited by the chemical method [8].

Publications devoted to chemical deposition of zinc sulfide films suggest reaction mixtures containing zinc salts, such as sulfate, chloride, or acetate, with ammonia and sodium citrate most frequently used as complexing agents. The role of a sulfidizer is, as a rule, played by thiocarbamide [9–12]. At the same tie, the formulations suggested for chemical deposition of ZnS films have not been substantiated, there is no scientific approach to the process in which zinc sulfide is obtained, and problems associated with the effect of the reaction mixture composition and substrate material on the composition and microstructure are not discussed.

The goal of our study was to prognosticate and assess the selection criteria of the component composition of the reaction mixture to be used for chemical deposition of nanostructured zinc sulfide films. It was also necessary to provide control over the nucleation process and to develop the required microstructure and composition of

a layer by using ligands with varied strength, zinc salts of varied nature, and various substrate materials.

EXPERIMENTAL

A objects of study served nanostructured zinc sulfide ZnS films produced by chemical deposition from aqueous solutions with the following salts: zinc chloride $ZnCl_2$ or zinc sulfide $ZnSO_4$ (both of chemically pure grade) and thiocarbamide N_2H_4CS (special-purity grade). An alkaline medium was created in the system by introduction of an aqueous solution of ammonia NH_4OH or sodium hydroxide in the reaction mixture. To make slower the formation rate of the ZnS solid phase, zinc-complexing additives were additionally introduced into the solution: ammonia in the form of ammonium hydroxide NH_4OH (chemically pure grade) or citrate ions in the form of trisubstituted sodium citrate $Na_3C_6H_5O_7$ (special-purity grade). Zinc sulfide films were deposited onto preliminarily degreased 30 × 24 mm glass-ceramic substrates of ST-50-1 brand or 6 × 20 mm glass plates. The synthesis was performed in a TS-TB-10 thermostat at 348–368 K, with the temperature maintained within ±0.1°.

The thicknesses of the deposited films were measured with a MII-4M Linnik microinterferometer.

The structural-morphological characteristics and the elemental composition of the films were examined with a JEOL JSM-5900 LV scanning electron microscope with an EDX attachment for energy-dispersive analysis (EDS Inca Energy 250 X-ray spectrometer). A MIRA3LMV microscope served to obtain electron-microscopic images with magnifications of 1000 to 100 000 at an electron beam accelerating voltage of 10 kV.

The crystal structure of the films was determined by X-ray diffraction analysis. The crystal structure of ZnS films was examined with an Empyrean X-ray diffractometer having unique performance capabilities, with a vertically arranged high-resolution goniometer. The X-ray measurements were made by the Bragg–Brentano method with Cu$K_{\alpha 1,2}$ radiation in the 2θ angle range 15–100° with a step Δ(2θ) = 0.02° and exposure of 15 s at a point. The phase composition of the samples and crystal lattice constants were determined and the structure of zinc sulfide films was finally refined by Rietveld's full-profile analysis method [13] with a FullProff software package.

RESULTS AND DISCUSSION

The process in which zinc sulfide films are obtained by hydrochemical deposition can be regarded as a set of topochemical reactions whose rate and mechanism are determined by the conditions created in the reactor [14]. The resulting chemical reaction of synthesis can be represented as:

$$ZnL_x^{2+} + N_2H_4CS + 4OH^- = ZnS\downarrow + xL + CN_2^{2-} + 4H_2O. \quad (1)$$

To decelerate the chemical precipitation of the metal sulfide phase to create conditions for film nucleation and formation, the metal should be preliminarily bound into complexes, which is provided by using complexing additive of varied strength and concentration in the course of synthesis. Undoubtedly, their chemical nature largely determines the rate and mechanism of the film-formation process, and determining the fundamental aspects of this influence will make it possible to control the growth process of a film and prognosticate its microstructure, morphology, and properties.

A procedure for calculating the boundary conditions and the concentration range in which the solid phase of a metal sulfide is deposited in relation to the pH value and complexation intensity has been developed and tested for a number of reaction systems. This procedure is based on an analysis of ionic equilibria in the reaction system and on the reversible type of decomposition of the chalcogenizer [14–16]. In this case, by the boundary deposition conditions is meant the dependence of the minimum content of a metal salt at which its conversion to a sulfide begins on the pH value of the reaction mixture.

The boundary conditions of deposition of the solid phase in dilute solutions are satisfied when the ionic product (IP) is equal to the solubility product (SP) of the metal chalcogenide. For example, for the poorly soluble zinc sulfide ZnS to be formed by reaction (1), is necessary that the following condition should be satisfied:

$$IP_{ZnS} = SP_{ZnS}, \quad (2)$$

where IP_{ZnS} is the ionic product, i.e., the product of the activities of the uncomplexed form of the metal (Zn^{2+}) and sulfide ions (S^{2-}); and SP_{ZnS} is the solubility product of the ZnS solid phase, which is a constant at a given temperature.

However, a stable formation of the solid phase by the homogeneous mechanism requires that a certain supersaturation in ZnS, manifested in the IP_{ZnS}/SP_{ZnS} ratio, should be created for compensating the excess surface energy of nuclei being formed and of the subsequent growth of particles of the new phase.

The extent of the supersaturation created in the system depends on the concentration of free Zn^{2+} ions in the volume of the reaction mixture. The stronger the supersaturation, the lower the Gibbs energy of nucleation, and the smaller the nuclei capable of further growth. In turn, the concentration of free zinc ions in the reactor volume is determined by the nature of the ligands being present. To assess their role and influence, we deposited ZnS films from citrate and ammonia reaction systems containing, respectively, zinc-complexing citrate ions $C_6H_5O_7^{3-}$ and ammonia NH_3.

The fraction of uncomplexed (active) zinc ions Zn^{2+} capable of entering into a chemical reaction with sulfide ions can be estimated by the expression [17]:

$$\alpha_{Zn^{2+}} = \frac{[Zn^{2+}]}{c_{Zn}} = \frac{1}{1+\frac{[L_1]}{k_1}+\frac{[L_1]^2}{k_{1,2}}+\quad+\frac{[L_1]^n}{k_{1,2,\ldots,n}}}, \quad (3)$$

where c_{Zn} is the total analytical concentration of zinc ions in solution; [L],concentration of the free ligand; and k_1, $k_{1,2}$, $k_{1,2,\ldots,n}$, instability constants of various complex forms of the metal.

We used in our calculations the following values of the instability constants of complex zinc ions: $pk_1 = 4.25$ for monodentate $ZnCit^-$, $pk_2 = 7.44$ for bidentate $ZnCit_2^{4-}$ in citrate complexes, $pk_3 = 10.92$ for mixed hydroxide-citrate complex $Zn(OH)Cit^{2-}$ [18]; $pk_4 = 2.18$, $pk_5 = 4.43$, $pk_6 = 6.93$, $pk_7 = 9.08$, $pk_8 = 9.46$, $pk_9 = 12.75$ for complexes with ammonia $ZnNH_3^{2+}$, $Zn(NH_3)_2^{2+}$, $Zn(NH_3)_3^{2+}$, $Zn(NH_3)_4^{2+}$, $Zn(NH_3)_5^{2+}$, $Zn(NH_3)_6^{2+}$ [19]; $pk_{10} = 6.04$, $pk_{11} = 11.1$, $pk_{12} = 13.6$, $pk_{13} = 14.6$ [19] for, respectively, the hydroxo complexes $Zn(OH)^+$, $Zn(OH)_2$, $Zn(OH)_3^-$, $Zn(OH)_4^{2-}$.

To determine the complex forms that are predominant in solution and exert a key influence on the deposition rate, we analyzed the ionic equilibria in the Zn^{2+}–$C_6H_5O_7^{3-}$–OH^- and Zn^{2+}–NH_3–OH^- systems.

The diagrams of distribution of the fraction concentrations of various complex forms of zinc in an aqueous solution for the ammonia and citrate systems on the pH value are shown in Fig. 1.

The results obtained in calculations of the ionic equilibria demonstrated that, with ammonia used as ligands, the fraction of zinc hydroxo complexes is rather insignificant: at pH < 13.0, their fraction is about 0.01. Using citrate ions as complexing agents for zinc, we can raise the fraction of hydroxo complexes being formed to 0.05 for $Zn(OH)_2$ in the pH range from 12.75 to 13.25 and to 0.35–0.38 for $Zn(OH)_3^-$ at pH of 12.75 to 13.25. It is noteworthy that the complex ion $Zn(OH)_4^{2-}$ is prevalent at pH 13–134, with its fractional concentration reaching a value of 0.65–0.94.

The main complexes hindering the fast precipitation of zinc sulfide in the system constituted by a zinc salt, ligand, and N_2H_4CS–OH^- at a pH value favorable for decomposition of thiocarbamide (10–13) are $Zn(NH_3)_6^{2+}$ (Fig. 1a) and $Zn(OH)Cit^{2-}$ (Fig. 1b).

It is possible that, in addition to the metal sulfide, impurity phases of zinc cyanamide and hydroxide can be formed in the reaction mixture and the content of these phases should be taken into account because a high supersaturation level is created for most of these because of their poor solubility. To determine the concentration ranges of existence of zinc sulfide and accompanying impurity phases in the systems under study, we calculated the boundary formation conditions by analyzing the ionic equilibria. To determine the minimum necessary concentration of the zinc salt, which provide formation of the ZnS solid phase in the reaction conditions under study in the presence of various complexing additives, we used the expression [14]:

$$pc_{in} = pSP_{ZnS} - p\alpha_{Zn^{2+}} - (pk_{H_2S} - 2pH + 0.5pK_c + p[N_2H_4CS]_{in} + 0.5p\frac{\beta_{cyan}}{\beta_S}) - \frac{0.86\sigma V_m}{RTr_{cr}}, \quad (4)$$

where p is the index (negative decimal logarithm); c_{in} , minimum initial concentration of the zinc salt, necessary for the ZnS solid phase to be formed; SP_{ZnS} , solubility product of zinc sulfide ($pSP_{ZnS} = 23.80$ [19]); $\alpha_{Zn^{2+}}$, the fractional concentration of free metal ions capable of entering into a chemical reaction; k_{H_2S} , ionization constant of hydrogen sulfide, one of thiocarbamide decomposition products ($pk_{H_2S} = 19.88$ [19]); K_c, hydrolytic decompo-

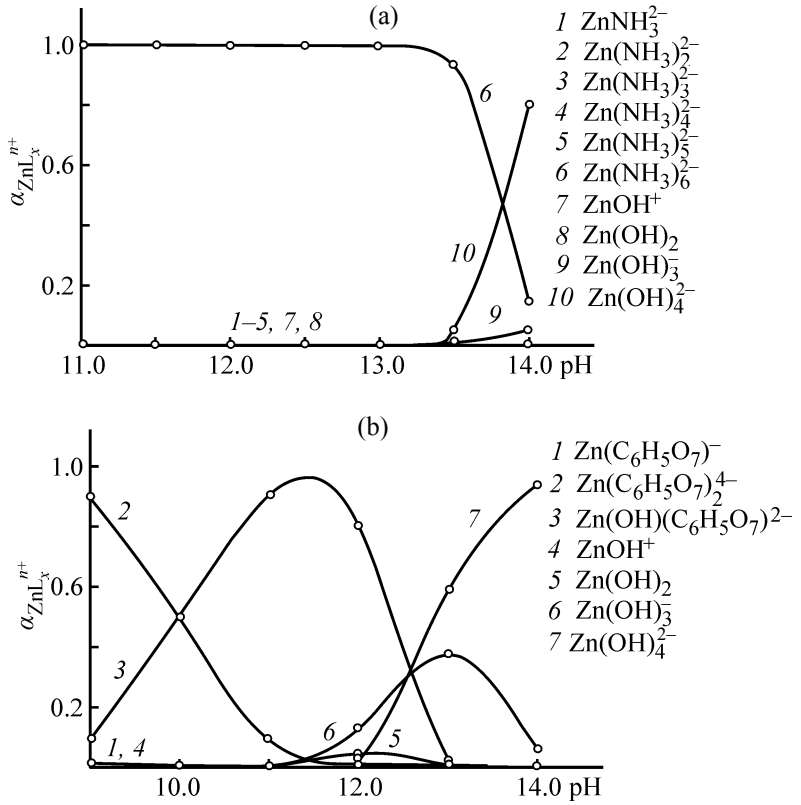

Fig. 1. Distribution diagrams of complex forms of zinc in (a) Zn^{2+}–NH_3–OH– and (b) Zn^{2+}–$C_6H_5O_7^{3-}$–OH– reaction systems. The initial concentration of a zinc salt is 0.1 M. ($\alpha_{ZnL_x^{n+}}$) Fraction.

sition constant of thiocarbamide (pK_c = 22.48 [14]); $[N_2H_4CS]_{in}$, initial concentration of the chalcogenizer (thiocarbamide) in solution, 0.6 M; σ, specific surface energy of zinc sulfide (1.0 J m^{-2}); V_m, molar volume of zinc sulfide (2.28×10^{-5} m^3 mol^{-1}); r_{cr}, radius of a critical-size nucleus (3.2×10^{-9} m); R, universal gas constant 8.314 J mol^{-1} K^{-1}; T, process temperature (353 K); β_S and β_{cyan} are given by $\beta_S = [H_3O^+]^2 + k_{HS^-}[H_3O^+] + k_{H_2S}$ and $\beta_{cyan} = [H_3O^+]^2 + k_{HCN_2^-}[H_3O^+] + k_{H_2CN_2}$, where k_{HS^-} and $k_{HCN_2^-}$ are the first-stage ionization constants of hydrosulfuric acid and cyanamide (pk_{HS^-} = 6.99 [19], $pk_{HCN_2^-}$ = 10.33 [14]); and $k^{1,2}_{H_2CN}$, the overall double-stage decomposition constant of cyanamide ($pk^{1,2}_{H_2CN_2}$ = 21.52 [14]) and hydrogen sulfide ($pk^{1,2}_{H_2S}$ = 19.88 [19]).

The last summand in expression (4) is derived from the Thomson–Ostwald relation and determines the contribution from the supersaturation in ZnS in the system with consideration for the formation of critical-size nuclei.

To calculate the boundary conditions of zinc cyanamide formation, we used the previously derived equation [16]:

$$pc_{in} = pSP_{ZnCN_2} - p\alpha_{Zn^{2+}} - \left(pk^{1,2}_{H_2CN_2} - 2pH_{in} + 0.5pK_c + 0.5p[N_2H_4CS]_{in} + 0.5p\frac{\beta_S}{\beta_{cyan}}\right), \quad (5)$$

where pSP_{ZnCN_2} is the solubility product index of zinc cyanamide (14.1 [14]).

The minimum concentration pcin of the zinc salt at which the formation of its hydroxide phase is provided was also found using [16]:

$$pc_{in} = pSP_{Zn(OH)_2} - p\alpha_{Zn^{2+}} - 2pK_w + 2pH_{in}, \quad (6)$$

where $[SP_{Zn(OH)_2}$ is the solubility product index of zinc hydroxide (17.15 [19]), and K_w is the ionic product of water.

The results obtained in calculation of the boundary conditions and zinc sulfide and hydroxide precipitation ranges for the reaction systems under consideration are presented in Fig. 2 as 3D graphical dependences in the

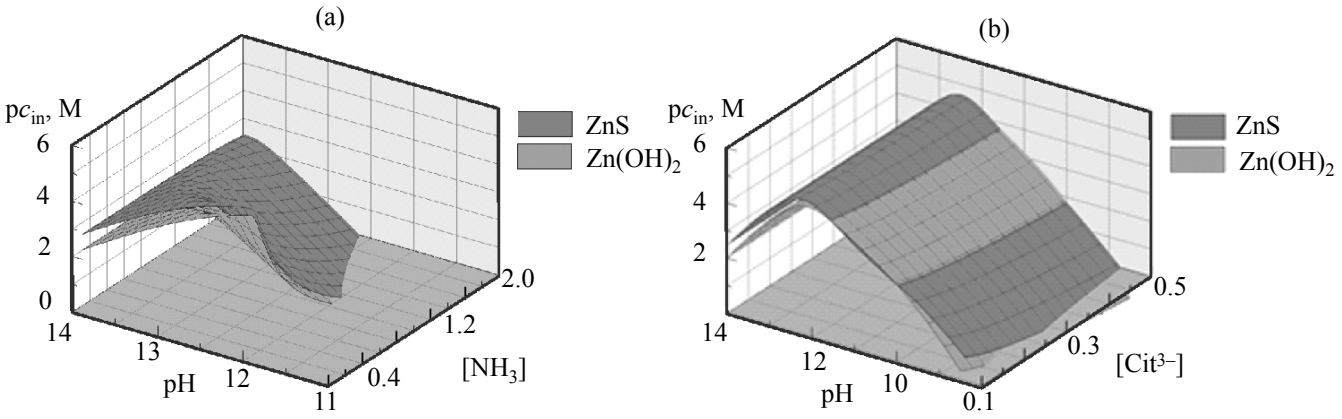

Fig. 2. Boundary conditions of zinc sulfide and hydroxide formation in (a) Zn^{2+}–NH_3–N_2H_4CS–OH^- and (b) Zn^{2+}–$C_6H_5O_7^{3-}$–N_2H_4CS–OH^- systems. The initial concentration of a zinc salt is 0.1 M. ([NH_3], [Cit^{3-}]) Concentration.

initial metal salt concentration–concentration of the introduced ligand–solution pH coordinates. It can be seen from these results that the ZnS solid phase is potentially formed in the pH range 12.0–14.0 in the ammonia system (Fig. 2a) and at 8.5–14.0 in the citrate system (Fig. 2b). Raising the concentration of ligands in the reaction mixture expectedly leads to an increase in the concentration of the zinc salt, which provides formation of its sulfide.

It is known [14] that films are formed on an unactivated substrate only in the range in which a thermodynamically stable metal hydroxide is formed, i.e., the $Zn(OH)_2$ phase serves as a natural surface activator, and OH^- ions act as condensation centers. It can be seen in Fig. 2 that the hydroxide phase whose presence has a positive effect in the initial stage of sulfide formation appears at pH > 12 for the ammonia system and pH ≥ 8.5 for the citrate system.

Our calculations demonstrated that necessary conditions for the zinc cyanamide phase to be formed in the reaction mixtures under consideration are not created.

According to the results of our calculations, the pH range 12–14 is the most favorable for deposition of ZnS films in the ammonia mixture under study, and 8–14 for the citrate system. In this case, the higher the solution alkalinity, the lower the required minimum zinc salt concentration in solution. It is noteworthy that zinc sulfide is formed in the citrate system at pH 10–12 via sulfidization of zincs hydroxide. In the present study, we chose for obtaining zinc sulfide films in the ammonia system a less alkaline range (pH ~12) than that in the citrate reaction mixture (pH 14) at a total zinc salt concentration introduced into the reaction mixture of 0.1 M.

In the Thomson–Ostwald expression [20], the size of the critical nucleus is directly related to the degree of supersaturation. We calculated the supersaturations created in reaction mixtures with ammonia (9.9×10^4) and citrate system (5.7×10^3) used as ligands. It is noteworthy that films are formed in both systems under study under supersaturation conditions. It can be assumed that the process in which zinc sulfide is formed in the ammonia system will differ due to the stronger supersaturation from the citrate system in a larger number of nuclei and formation of smaller crystallites and, consequently, is characterized by the formation on a substrate of comparatively dense and structurally uniform film.

The supersaturation for the citrate system is an order of magnitude weaker than that for the ammonia system, and, consequently, particles forming the film will be coarser, and their number somewhat smaller. This must lead to an increase in existence time of the island structure of the film, and, consequently, to a less dense spatial packing by the time of completion of its synthesis.

In the course of a 2-h chemical synthesis occurring at 363 K in both the systems under study under the conditions chosen on the basis of the results of our calculations and preliminary experiments, we obtained even lustrous zinc sulfide layers uniformly covering the surface of glass-ceramic and glass substrates with good adhesion to these substrates. The thickness of these layers was 200 to 240 nm, depending on the synthesis conditions.

The extent to which a zinc sulfide film is close to the stoichiometric composition is an important criterion of the optical quality of the material, which is provided, as

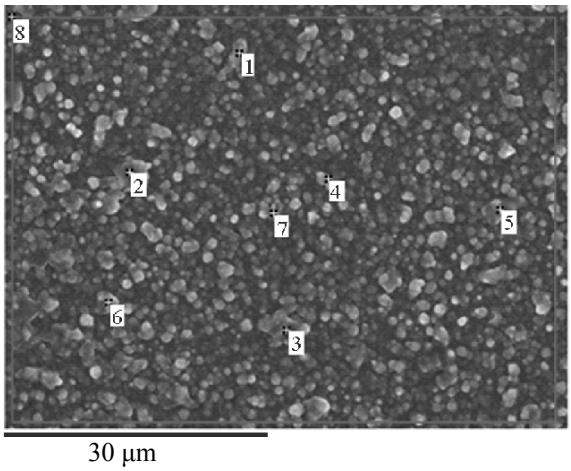

Spectrum	S	Zn
	at %	
1	51.88	48.12
2	51.11	48.89
3	50.24	49.76
4	49.28	50.42
5	49.26	50.74
6	51.49	48.51
7	53.67	46.33
8	48.34	51.66
Average	50.70	49.30

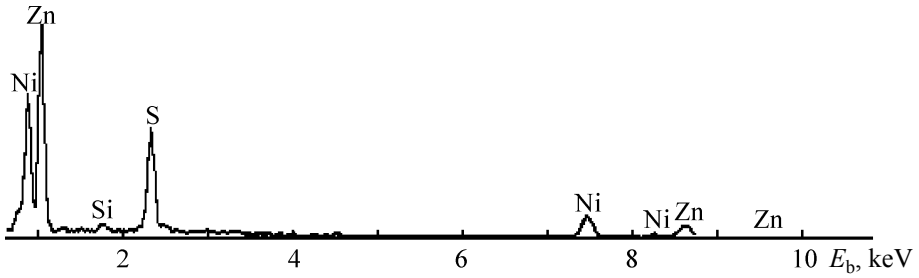

Fig. 3. Results of an elemental analysis of a ZnS film produced by chemical deposition from an ammonia reaction mixture containing zinc chloride. (E_b) Binding energy.

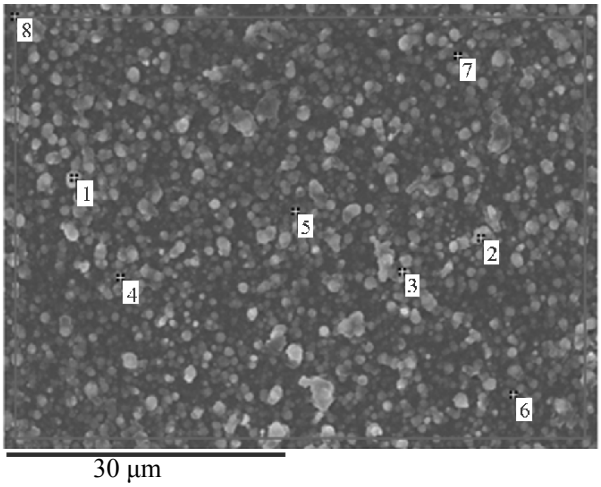

Spectrum	S	Zn
	at %	
1	47.34	52.66
2	48.26	51.74
3	47.72	52.28
4	48.13	51.87
5	47.59	52.41
6	45.82	54.18
7	47.72	52.28
8	45.87	54.13
Average	47.30	52.70

Fig. 4. Results of an elemental analysis of a ZnS film produced by chemical deposition from an ammonia reaction mixture containing zinc sulfate. (E_b) Binding energy.

noted in [21], in a low-temperature synthesis. In addition, films synthesized under sharply nonequilibrium conditions. This requirement is satisfied by the hydrochemical deposition used in the present study. However, an important factor affecting the stoichiometric composition of the sulfide under study is the zinc salt. The results of a comparative analysis of the elemental composition of zinc sulfide films synthesized at 368 K from reaction mixtures containing zinc chloride and sulfate as precursors are presented in Figs. 3 and 4.

The above results suggest that, to obtain a ZnS film with nearly stoichiometric composition, it is preferable to use the zinc chloride salt providing a Zn : S ratio of 49.3 : 50.7 in the deposited layer against 52.7 : 43.3 for the film obtained with zinc sulfate in the reaction mixture.

The films under study were subjected to an X-ray diffraction analysis in the conventional Bragg–Brentano configuration. The glancing beam method was used, in which the surface of a film under study is arranged at a small angle (1°) to the incident beam and its position remains unchanged in the course of exposure to exclude reflections from the glass-ceramic substrate. Analysis of the X-ray diffraction pattern of a zinc sulfide film produced by chemical deposition from an ammonia reaction mixture containing zinc chloride (Fig. 1) unequivocally demonstrates that the film contains only crystal phase of ZnS. In turn, the presence of a strong reflection at $2\theta = 29.78°$ shows that the deposited zinc sulfide layer has a cubic sphalerite modification with lattice constant $a = 0.5315$ nm (JCPDS card no. 79–0043) [22–26].

The intensity ratio of crystallite reflections, observed in the X-ray diffraction pattern of the sample under study, is indicative of their preferable orientation in the direction of the (111) face. It was reported in [27] that crystals with the [111] orientation are more preferable as regards optical properties.

Electron-microscopic images of zinc sulfide layers produced with various metal salts by chemical precipitation from ammonia and citrate reaction mixtures are presented in Figs. 6 and 7. Their comparison shows in all cases significant differences in the morphology of the deposited films. It should be noted, however, that, irrespective of the kind of a reaction mixture, the main structural elements are predominantly spherical aggregates having the form of a set of finer particles of globular shape characteristic of zinc sulfide [28].

Figure 6 shows electron-microscopic images of ZnS layer produced at 353 K from a citrate reaction mixture, with zinc chloride or sulfate used as a zinc salt. It can be summarized that the nature of a salt being used strongly affects the morphology of these films. Films obtained with zinc chloride are rather homogeneous and densely packed, with the predominant particle diameter of 30–50 nm. By contrast, the layers obtained with $ZnSO_4$ are less uniform in the size of the constituent crystallites and visually have a looser structure. These layers are based, on the one hand, on nanoparticles with sizes of about 30–40 nm and, on the other hand, on their aggregates with diameters of up to 400 nm, probably formed in solution and then adsorbed therefrom in the final stage of synthesis.

Figure 7 shows electron-microscopic images of zinc sulfide films on glass-ceramic substrates, deposited from the ammonia (a) and citrate (b) systems at 368 K in the course of 120 min. Zinc sulfate served as the zinc salt. It can be seen that, in both cases, the appearing spherical primary particles with sizes of 20–30 nm form large-size globular aggregates. Their diameters and morphological features are noticeably different, depending on the reaction system used. For example, their predominant sizes are 200–600 nm in the ammonia system, and 150–400 nm, i.e., 1.5 times smaller, in the citrate system. The shape of the particles has elements of faceting in the first case.

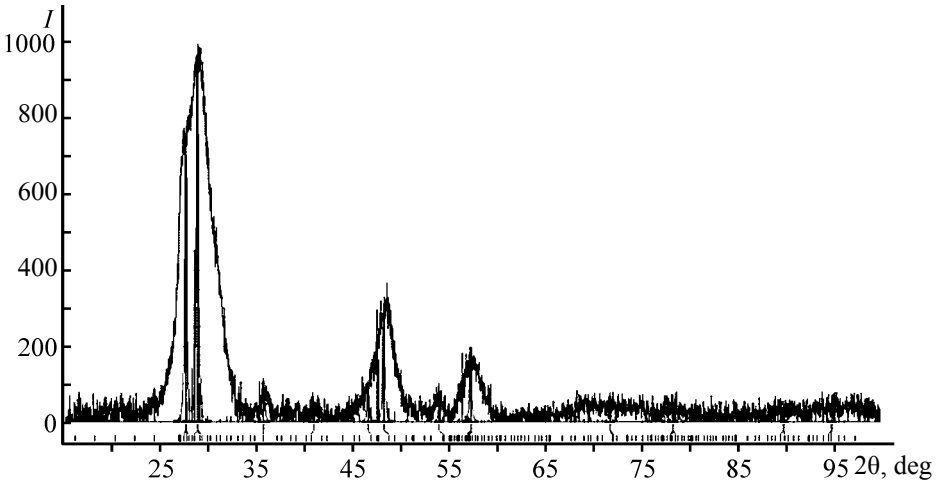

Fig. 5. Diffraction reflections from a ZnS film produced by chemical deposition on a glass-ceramic substrate from an ammonia reaction mixture containing zinc sulfate. Deposition duration 120 min, process temperature 368 K. (*I*) Intensity and (2θ) Bragg angle.

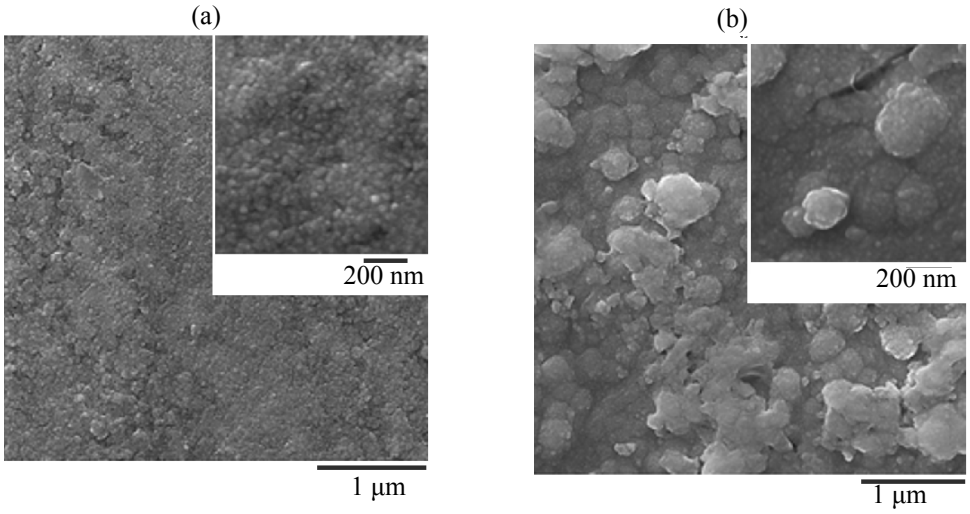

Fig. 6. Electron-microscopic images of ZnS films deposited in the course of 120 min on glass-ceramic substrates from a reaction mixture containing (a) zinc chloride and (b) zinc sulfate. Synthesis temperature 353 K.

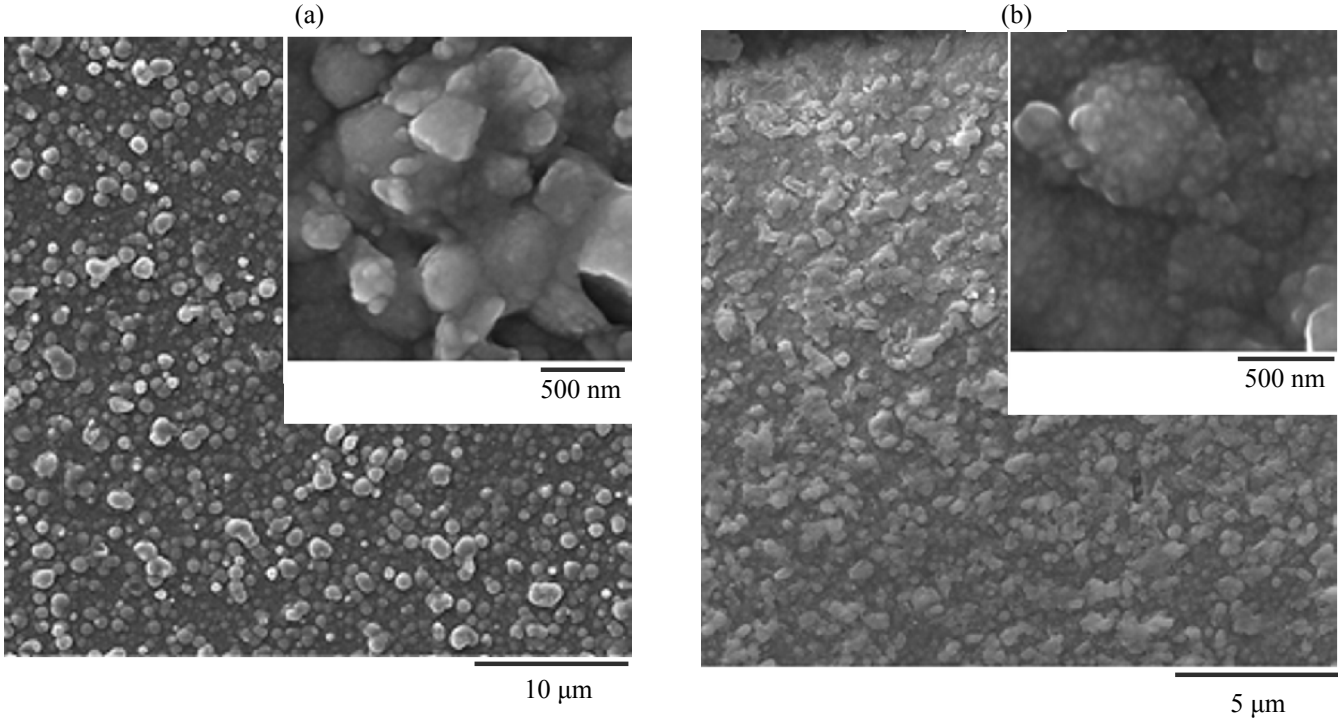

Fig. 7. Electron-microscopic images of zinc sulfide films on glass-ceramic substrates, deposited from (a) ammonia and (b) citrate systems at 368 K in the course of 120 min. The reaction mixture contained $ZnSO_4$ as the zinc salt.

We analyzed the influence exerted by the substrate material on the morphology of chemically deposited ZnS films. Figure 8 shows for comparison electron-microscopic images of the films on glass (a) and glass-ceramic (b) substrates. It can be seen that the physicochemical nature of the material of a substrate and the nature of its surface largely determine the morphology of the deposited layers. The film formed on the glass substrate has a more homogeneous fine-grained structure with particle sizes of 50–150 nm. This film has on its surface coarser inclusions with diameters of up to 400 nm, probably formed as a result of adsorption from the bulk of the reaction mixture.

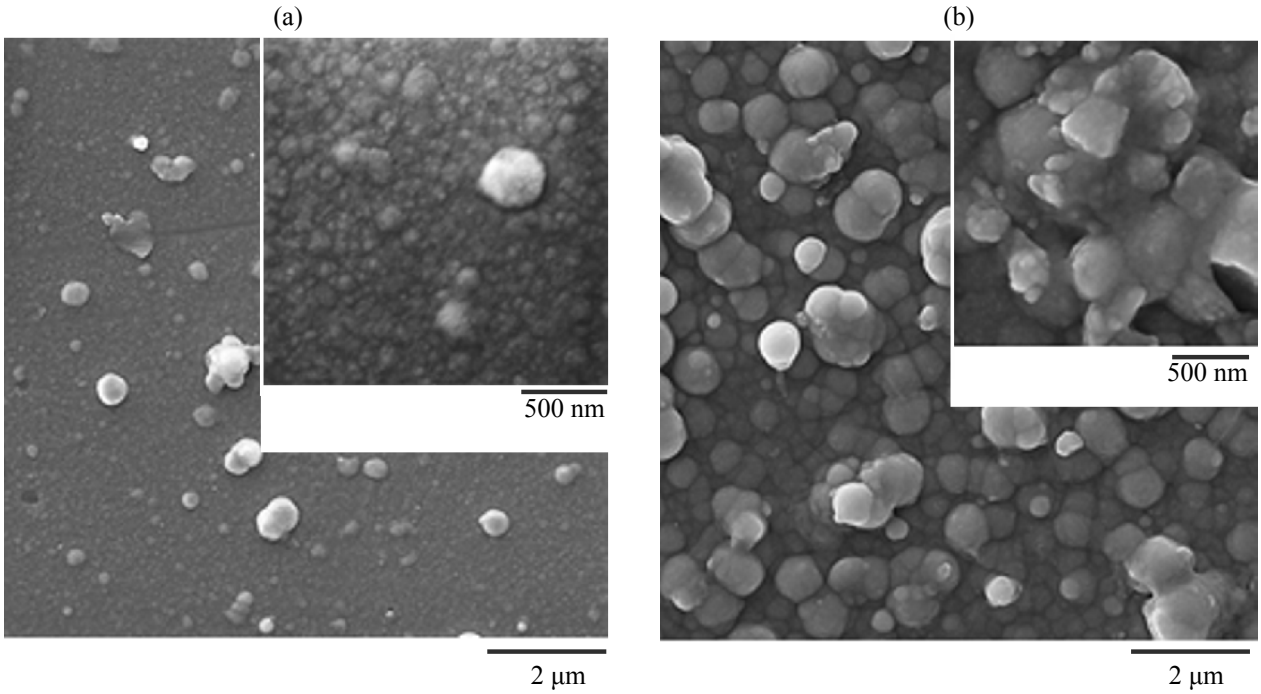

Fig. 8. Electron-microscopic images of zinc sulfide films produced by chemical deposition from an ammonia system at 368 K in the course of 120 min on (a) glass and (b) glass-ceramic substrates, with the reaction mixture containing zinc sulfate $ZnSO_4$.

An analysis of the surface morphology of ZnS films obtained on the glass-ceramic substrate demonstrated that these films are composed of globules with rather widely varying sizes: from 100 to 600 nm. A detailed consideration of these globules suggests that they are aggregates of spherical particles up to 50 nm in size. The specific features of the morphology of films on the glass-ceramic substrate are due, in our opinion, to the stronger chemical and geometrical nonuniformity of its surface.

The influence exerted on the morphology of ZnS films by the synthesis temperature in the range 353–368 K in deposition from the ammonia system onto a glass substrate is illustrated by Fig. 9. The above electron-microscopic images suggest that raising the deposition temperature within the above range enhances the granulometric inhomogeneity of a film being synthesized and leads to a certain increase in the average size of its constituent crystallites.

Analysis of the data on the morphological specific features of the ZnS films, obtained in the present study, largely confirms our earlier concepts about the growth mechanism of metal chalcogenide films in their hydrochemical deposition on the scale hierarchy principle [14, 15]. Based on the above data, we can distinguish the following main growth stages of the films under study: formation of critical-size nuclei on the substrate surface, their growth accompanied by merging of island formations, and growth of a film via adsorption of particles chaotically moving as a result of the Brownian motion from the solution bulk.

Our experimental data demonstrated that an important role is played, together with the complexation process determining the supersaturation with respect to ZnS, by the anionic component of the metal salt used in the reaction mixture. The varied spatial structure of the anionic component of a salt can strongly affect the behavior of primary clusters in a growing film, with their mutual collisions in the bulk of the reaction mixture and with the film surface hindered or blocked. Indeed, layers deposited with $ZnSO_4$ in the presence of sulfate ions having a rather developed spatial structure have a less dense and less ordered particle arrangement as compared with a film deposited from a zinc chloride solution.

The morphology of ZnS films being deposited is determined by the strength and content of complexing additives in the reaction mixture, zinc salt used in synthesis, nature of the substrate material, and synthesis process temperature.

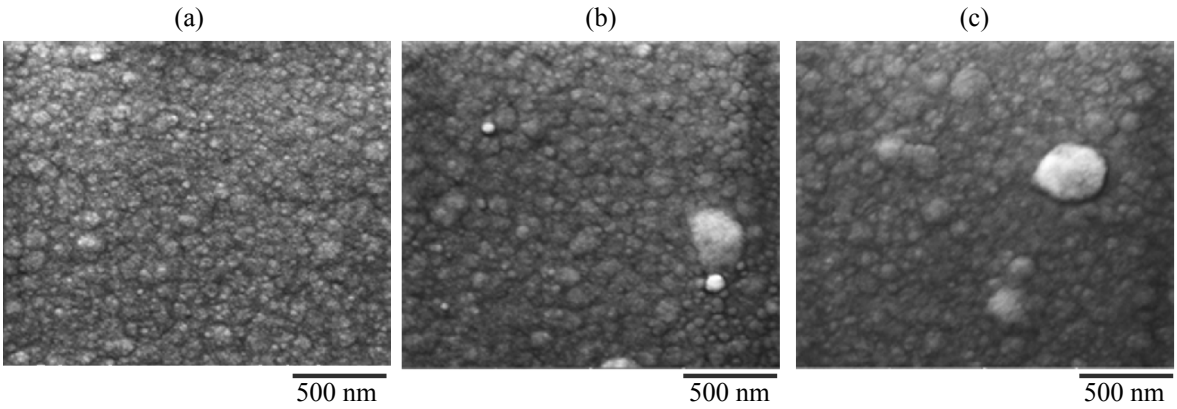

Fig. 9. Electron-microscopic images of ZnS films deposited in the course of 120 min from an ammonia system on a glass substrate at temperatures of (a) 353, (b) 358, and (c) 368 K. The deposition was performed from the reaction mixture containing zinc sulfate.

CONCLUSIONS

(1) The boundary conditions and formation ranges of zinc sulfide and accompanying phases [$Zn(OH)_2$, $ZnCN_2$] were determined by calculation.

(2) The hydrochemical deposition at 363 K from citrate and ammonia systems was used to synthesize nanostructured zinc sulfide films with thicknesses of 200 to 240 nm on glass and glass-ceramic substrates.

(3) An analysis made in the study demonstrated that the ZnS films have a cubic sphalerite structure with predominant sizes of structured particles of 50–150 nm on glass substrates and 100–600 nm on glass ceramics.

(4) It was found that the anionic component of a salt being used exerts a key influence on the morphology and spatial structure of the ZnS films.

ACKNOWLEDGMENTS

The study was supported by Program 211 of the Government of the Russian Federation (no. 02.A03.21.0006) and by the Ministry of Education and Science of the Russian Federation under the state assignment no. 4.1270.2014/K.

REFERENCES

1. Sorokin, E., Naumov, S., and Sorokina, I.T., *IEEE J. Sel. Top Quant. Electron*., 2005, vol. 11, no. 3, pp. 690–712.
2. Park, S., Kim, H., Jin, C., and Lee, C., *Current Appl. Phys*., 2012, vol. 12, no. 2, pp. 499–503.
3. Chopra, K.L. and Das, S.R., *Thin Film Solar Cells,* New York: Plenum Press, 1983.
4. Dharmadasa, I.M., *Advances in Thin Film Solar Cells*, Pan Stanford Publishing, Hardback, 2012.
5. Kashani, H., *Thin Solid Films*, 1996, vol. 288, nos. 1–2, pp. 50–56.
6. Opanasyuk, A.S., Kurbatov, D.I., Berestok, T.O., et al., *Vestn. Nats. Tekhn. Univ. Kharkov. Politekhn. Inst., Ser. Nov. Resheniya Sovr. Tekhnol*., 2013, no. 18 (991), pp. 149–155.
7. Klochko, N.P., Khripunov, G.S., Volkova, N.D., et al., *Fiz. Tekh. Poluprovodn.*, 2014, vol. 48, no. 4, pp. 539–548.
8. Maskaeva, L.N., Fedorova, E.A., Shemyakina, A.I., and Markov, V.F., *Butlerovskie Soobshch*., 2014, vol. 37, no. 2, pp. 1–9.
9. Liu Qi, Guobing Mao, and Jianping Ao, *Appl. Surf. Sci.,* 2008, vol. 254, no. 18, pp. 5711–5714.
10. Jie Cheng, DongBo Fan, Hao Wang, et al., *Semicond. Sci. Technol.*, 2003, vol. 18, no. 7, pp. 676–681.
11. Ben Nasr, T., Kamoun, N., Kanzari, M., et al., *Thin Solid Films*, 2006, vol. 500, pp. 4–8.
12. Huda Abdullah, Norhabibi Saadah, and Sahbuddin Shaari, *World Appl. Sci. J.*, 2012, vol. 19, no. 8, pp. 1087–1091.
13. Rietveld, H.M., *J. Appl. Crystallogr.*, 1969, vol. 2, no. 2, p. 65.
14. Markov, V.F., Maskaeva, L.N., and Ivanov, P.N., *Gidrokhimicheskoe osazhdenie plenok sul'fidov metallov: modelirovanie i eksperiment* (Hydrochemical Deposition of Metal Sulfide Films: Simulation and Experiment), Yekaterinburg: Ural. Otd. Ross. Akad. Nayuk, 2006.
15. Markov, V.F., Maskaeva, L.N., Loshkareva, L.D., and Uimin, S.N., *Izv. Ross. Akad. Nauk, Neorgan. Mater.*, 1997, vol. 33, no. 6, pp. 665–669.
16. Markov, V.F. and Maskaeva, L.N., *Russ. J. Phys. Chem.,* 2010, vol. 84, no. 8, pp. 1288–1293.
17. Butler, J.N., *Ionic Equilibrium,* Ner York: Wiley, 1964.
18. Zhivopistsev, V.P. and Selezneva, E.A., *Analiticheskaya khimiya tsinka* (Analytical Chemistry of Zinc), Moscow: Nauka, 1975.

19. Lur'e, Yu.Yu., *Spravochnik po analiticheskoi khimii* (Handbook of Analytical Chemistry), Moscow: Khimiya, 1989.
20. Frolov, Yu.N., *Kurs kolloidnoi khimii. Poverkhnostnye yavleniya i dispersnye sistemy* (A Course of Colloid Chemistry: Surface Phenomena and Dispersed Systems), Moscow: OOO Izd. Dom Al'yans, 2009.
21. Belyaev, A.P., Rubets, V.P., Nuzhdin, M.Yu., and Kalinkin, I.P., *Fiz. Tekh. Poluprovodn*., 2003, vol 37, no. 6, pp. 641–643.
22. Ashrat, M., Mehmood, M., and Qayyum, A., *Fiz. Tekh. Poluprovodn.*, 2012, vol. 46, no. 10, pp. 1349–1352.
23. Huda Abdullah, Norhabibi Saadah, and Sahbuddin Shaari, *World Appl. Sci. J*., 2012, vol. 19, no. 8, pp. 1087–1091.
24. Eman M. Nasir, *Int. J. Innovative Res. Sci. Eng. Technol.,* 2014, vol. 3, no. 1, pp. 8114–8120.
25. Bhupender Pal and Bonamali Pal, *Chem. Eng. J.*, 2015, vol. 263, pp. 200208.
26. Valeev, R.A., Beltyukov, A.N., Gilmutdinov, F.Z., et al., *J. Struct. Chem.*, 2011, vol. 52, Suppl., pp. 181–186.
27. Krasnoperova, A.P., Belikov, K.N., Sofronov, D.S., et al., *Metody Ob"ekty Khim. Analiza*, 2013, vol. 8, no. 4, pp. 194–198.
28. Markov, V.F. and Maskaeva, L.N., *Russ. Chem. Bull.*, 2014, no. 7, pp. 1523–1532.